Volumetric flow field measurements around a stepped cylinder with an object-aware Lagrangian particle tracking approach

Thomas Rockstroh[1,*]

1: LaVision GmbH, Anna-Vandenhoeck-Ring 19, 37081, Göttingen, Germany
*Corresponding author: trockstroh@lavision.de

Keywords: PTV, LPT, Shake-the-Box, Objects, FSI

ABSTRACT

Instantaneous, three-dimensional flow field measurements around cylindrical objects can pose special problems for the experimental set-up due to the complex camera set-up required to image the complete measurement domain. Recently, a novel Object-aware Shake-the-Box (OA-STB) has been proposed to integrate object information in the particle triangulation step for Lagrangian particle tracking (LPT) methods. Within this conference paper, a validation experiment of this novel OA-STB implementation is presented with the motivation of providing data analysis details and to serve as a guideline for future measurements of a similar scope. The reconstruction quality of the object aware particle triangulation is analyzed with respect to the estimated measurement uncertainties. Further, a single exemplary trajectory is considered in order to investigate, whether nonphysical discontinuities occur, when a particle crosses differently imaged regions.

1. Introduction

The flow past a cylinder is a very thoroughly and widely investigated canonical flow configuration. Besides interesting aspects for fundamental research, it is also of a very practical and technical relevance. From a metrological point of view, many studies already incorporated non-invasive flow measurements, such as planar Particle Image Velocimetry (PIV) (Perrin et al., 2008; Zhang et al., 2005; Zhou et al., 2015) or volumetric tomographic PIV (Tomo-PIV) (Crane et al., 2022; Hain et al., 2008), to investigate this type of flow. But when it comes to optical measurement techniques, one has to always work around certain restrictions with respect to optical accessibility and should aim to minimize shadowed and or occluded measurement regions. In experimental set-ups, where it is possible to view along the cylinder's axis it is quite easy to not only image the wake of the cylinder but also to simultaneously capture the upstream regions and the near-wall flow. But in cases, where the cylinder's axis has to be placed perpendicular to the camera's line-of-sights, more hardware is required, since cameras have to be placed all around the cylinder to capture both

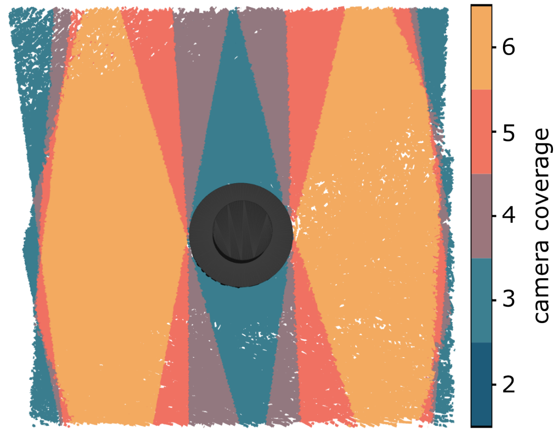

Figure 1. Schematic illustration of differently covered regions for an experimental set-up with a total of six cameras placed in groups of three on two sides of a cylinder.

the up- and downstream regions. As a result, there will be regions in the imaged measurement domain, which might be seen by all cameras, but which also might be seen by only a smaller sub set of cameras. Such a configuration is schematically shown in Figure 1 for an set-up of six cameras – which will later also be used in the here presented experiments.

Now, when dealing with such data, the flow reconstruction algorithm should be capable of properly handling these different regions. For Tomo-PIV this would require, that a voxel's intensity only gets contributions from cameras, which are actually able to see this part of the volume and for Lagrangian particle tracking (LPT), the triangulation of a particle should only be possible from cameras, which line-of-sights intersect without interference from the obstructing object. In Shake-the-Box (STB) (Schanz et al., 2016), a 3D-LPT method based on the Iterative Particle Reconstruction (IPR) scheme (Wieneke, 2013), this special condition can be met indirectly by choosing a very loose set of IPR triangulation constrains. With this set of parameters, the reconstruction around an object is feasible but only at the cost of greatly increasing the chance of producing ghost particles in region of reduced camera coverage. As a proposal to improve the reconstruction quality of STB in such scenarios, a special object-aware Shake-the-Box (OA-STB) implementation was recently developed by Wieneke & Rockstroh (2024). For an experimental validation of this algorithm, flow field measurements around a view-obstructing stepped cylinder, featuring a six-camera set-up, were performed. Within this work, these measurements and the used experimental set-up will be described together with a presentation of the required data processing steps to proper utilize the novel OA-STB method. Reconstruction results, both particle trajectories and interpolated velocity fields, are shown. In addition, a focus on the consistency on the flow reconstruction results at the interfaces of the different camera coverage areas is set.

2. Experimental set-up

Experiments are performed in a rectangular water tank with the dimensions of (1000 × 400 × 400) mm, in which a stepped cylinder is placed in the center. The cylinder features two sections with different diameters, whereas the smaller diameter measures 30.5 mm and the larger diameter 55.9 mm. Flow within the tank is created with a commonly available aquarium pump with a circular orifice. The pump is oriented in a way, that the emitted jet directly impinges on the cylinder's surface. As flow tracers, fluorescent polyethylene particles (UVPMS-BO-1.00, Cospheric, 1000 kg m^{-3}) with a diameter of 125 – 150 µm are used. Illumination of the volume is provided by two pulsed LED arrays (LED 300 Flashlight, LaVision) set to a pulse length of 250 µs. In order to capture the complete flow field around the cylinder, six CMOS cameras (Imager CX-5, LaVision, 2440 × 2040 px, 300 µs exposure time) are placed on both sides of the tank in two groups of three. Using 28 mm focal length lenses (AF Nikkor 28mm/2.8 D, Nikon) at a f-stop value of 8 and Scheimpflug adapters (Scheimpflug adapter V3, LaVision), a common imaged volume of (240 × 200 × 300) mm is covered. Optical long-pass filters with a cut-on wavelength of 540 nm are placed in front of the lenses to block reflections and to minimize background signals from the LEDs. Time-resolved recordings covering 500 images are achieved with an image acquisition frequency of 120 Hz, resulting in maximum particle displacements of around 20 px. A photograph of the complete set-up is presented in Figure 2.

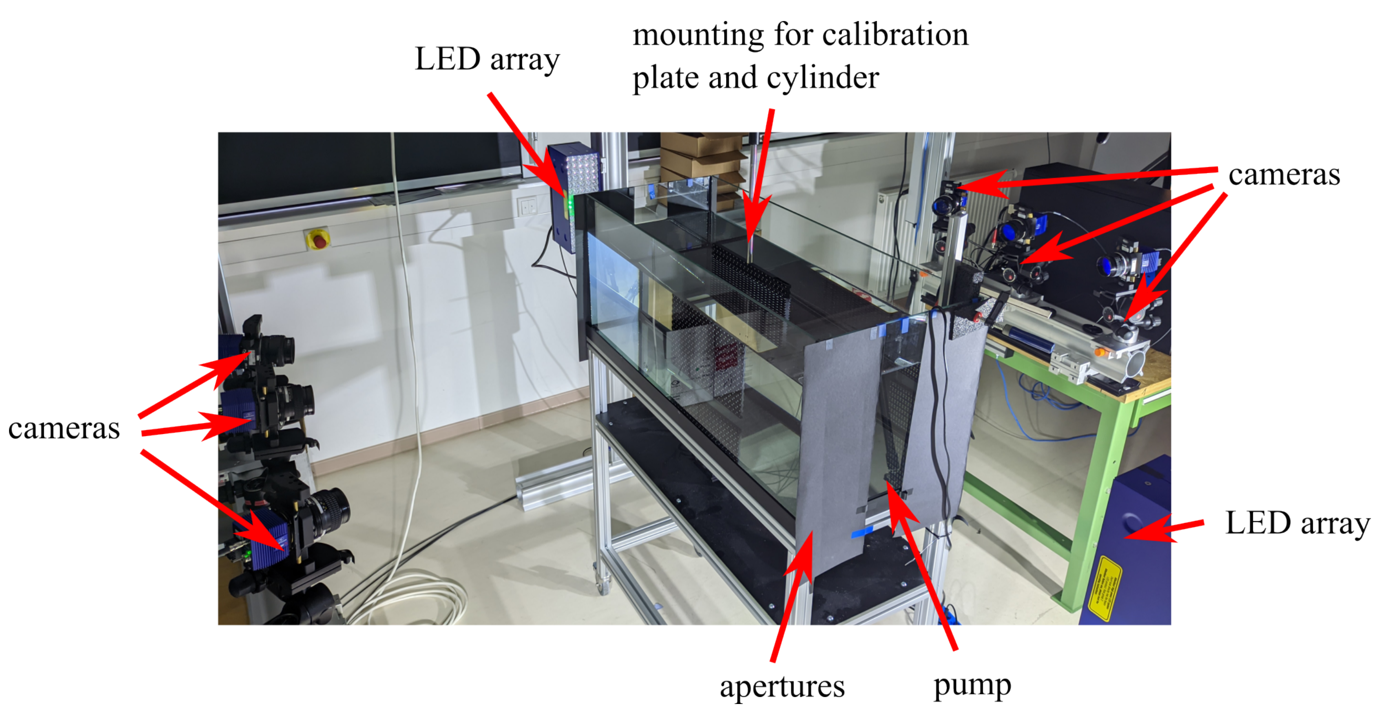

Figure 2. Photograph of the experimental set-up, consisting of the six-camera system, two LED arrays, mounting material for both the calibration plate and the stepped cylinder and the pump. Apertures are installed at the sides of the aquarium to produce a defined illumination volume.

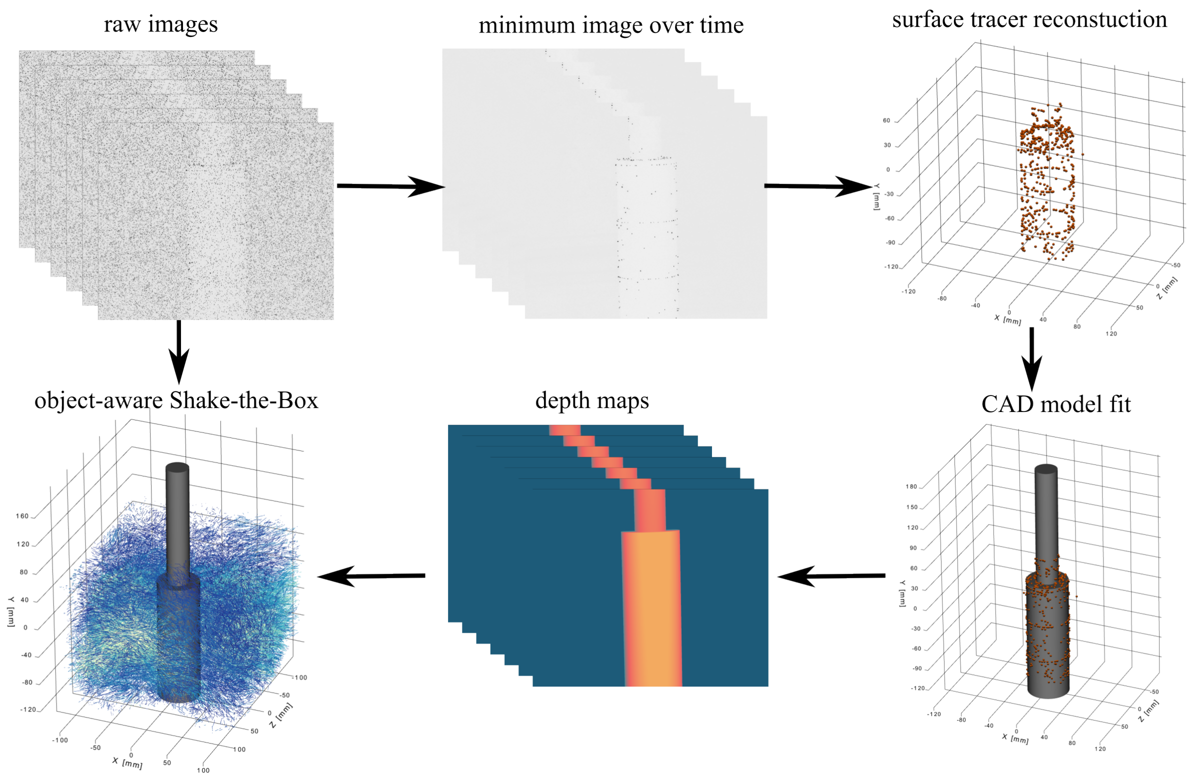

Figure 3. Processing workflow of the object-aware Shake-the-Box approach. Starting from the raw camera images, the stationary surface tracers are extracted and separately reconstructed. The resulting point cloud is used to fit the correct orientation of the cylinder's CAD model. After calibrating the camera system, the camera depth maps can be deduced from the CAD model. Finally, both the raw images and depth maps are taken to reconstruct the time-resolved three-dimensional particle trajectory with the novel object-aware Shake-the-Box scheme.

3. Data processing

The recorded images are evaluated with STB (Schanz et al., 2016) and it's novel object-aware extension OA-STB (Wieneke & Rockstroh, 2024) with the aim of recovering the time-resolved three-dimensional particle trajectories all around the cylinder. For this novel approach it is necessary to calculate a depth map for each camera. This depth map encodes the position of the obstructing cylinder in the reconstruction volume and defines the end of each pixel's line-of-sight. For a correct determination of the depth maps it is required, that the position of the object is known in the multi-camera coordinate system with sufficient accuracy (at least pixel accurate). In this work, the determination of the correct object position is done by utilizing the presence of stationary tracer particles attached to the cylinder's surface. Those tracer particles are separated from the moving flow tracers by a proper image pre-processing step, in which the minimum intensity image over the complete time series is calculated.

These minimum intensity images are then used as an input for an IPR step and the 3D position of the surface tracers is obtained. Since the object information is not available at this step, yet, IPR is used in the conventional implementation. In order to avoid confusions in the reconstruction process due to the obstructed views, the measurement system is split in two sub-groups for the surface tracer reconstruction. The first sub-group only uses the three cameras located on one side of the tank and the second one the three cameras on the opposing side. By combining both reconstruction results, the reconstruction of surface tracer particles all around the perimeter of the cylinder is finished.

With the help of the reconstructed point cloud, a CAD model of the stepped cylinder can be correctly positioned in the measurement volume. This can either be done manually or, more preferably, automatically using a point cloud registration method, such as the Iterative closest point (ICP) matching (Hendriksen et al., 2024). All necessary depth maps for the OA-STB approach are determined and can now be used together with the raw images as an input for the final STB analysis. The whole workflow is schematically depicted in Figure 3.

For the actual Shake-the-Box processing a variable time-step strategy (VT-STB) (Schanz et al., 2021) combined with a forward-backward tracking scheme is applied. In total five processing passes are performed, with decreasing image increments of 5, 3, 2, 1 and 1. Particles are detected in the images if their peak intensity is above 10 counts and the allowed triangulation error is set to 1 px. Particles are triangulated if they are observed by at least three cameras. The chosen IPR parameters are set to: 4 outer iterations, 4 inner iterations, shake distance of 0.1 voxel, particle duplicates are removed if they should occur within a 1 voxel distance and particles are filtered out from the reconstruction if their intensity drops below 20 % of the average intensity of all reconstructed particles. Trajectories are initialized with a maximum particle displacement of 20 voxel.

4. Results

Reconstructed particle trajectories during a time interval of 25 time steps are shown in Figure 4 left. The jet flow can be identified as well as the flow separation around the cylinder. The reconstruction results show a completely reconstructed measurement volume without obvious reconstruction artifacts introduced by the occluding object. In total, 229854 trajectories are reconstruction during the complete image sequence of 500 images. On average, 29915 particles are simultaneously tracked per time step and the average track length is 65 time steps. An interpolated velocity field at time step 250 is presented in Figure 4 right. The velocity field is calculated by binning the particle tracks with a bin size of (128 x 128 x 128) vox and a 75% overlap. The shown vector field originates from a XZ-slice through the volume at Y = -50 mm. Vortical flow structures are identified by iso-surfaces of the λ_2 criterion at a threshold of 5 1/s. The vector field indicates an asymmetric impingement of the jet, which features turbulent flow structures already upstream of the cylinder.

As a next result, all of the trajectories are analyzed with respect to their estimated position and velocity uncertainties in the different regions of the measurement domain categorized by the camera

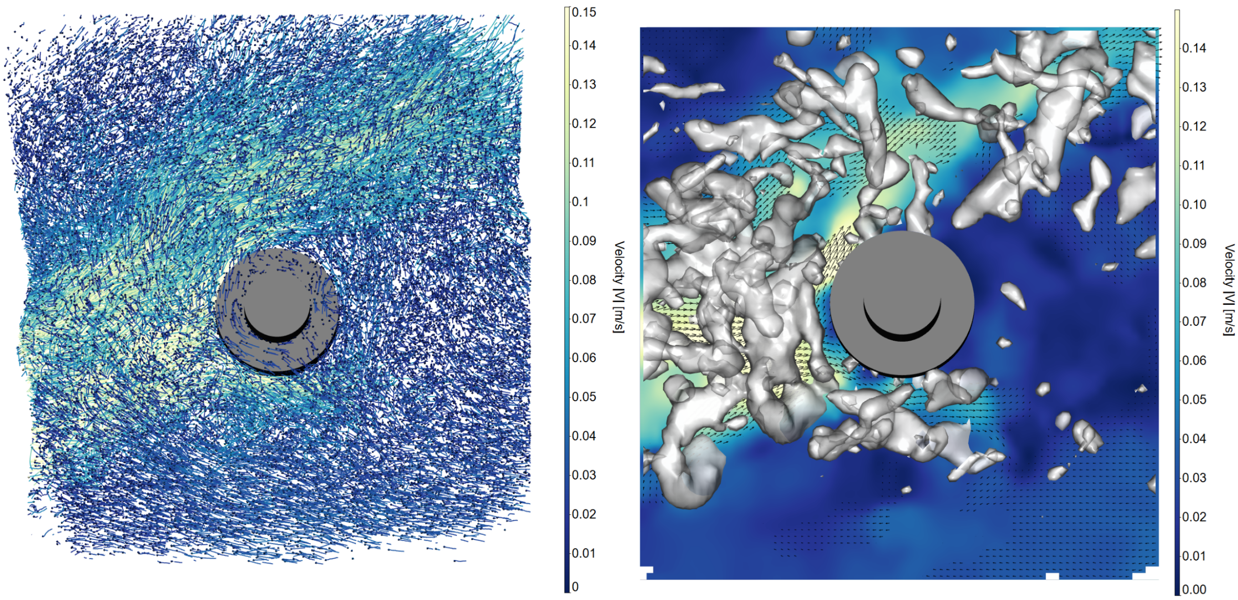

Figure 4. Reconstruction results from the object-aware Shake-the-Box calculations. Left: Particle trajectories centered around time step 250 with a drawn trail length of 25 time steps. Color-coding of the tracks represents the local stream-wise velocity. Right: Interpolated velocity field at time step 250 with a XZ-slice at Y = -50 mm through the volume showing the velocity magnitude. Vortical structures are represented as white iso-surfaces of the λ_2 criterion at a threshold of λ_2 = 5 1/s.

coverage, i.e. the number of cameras able to see a certain region. For this purpose, the uncertainties for every particle present the reconstruction are estimated from a fixed-width (11 time-steps) 2nd order polynomial regression and from an adaptive 2nd order polynomial regression (Janke & Michaelis, 2021)). Box plot visualizations of the resulting uncertainty distributions are presented in Figure 5.

Overall, the median uncertainty values for each of the different camera coverage areas are very similar but the widths of the distributions tend to decrease significantly with a higher number of cameras observing a certain measurement region. With respect to the position uncertainties, the estimated median values are between 6-10 µm, resulting in unscaled uncertainties (scaling factor of this experiment: 12.41 px/mm) of 0.07-0.12 px. The relative velocity uncertainties appear to be more influenced by the number of cameras able to cover certain measurement regions, where the scatter of the data for a camera coverage of 3 is roughly 3-4 times higher than the data for a camera coverage of 6. Median values for U_w/u_{abs} of all presented distributions are between 0.3-0.8 %. This is most likely caused by the fact, that all of the regions with a camera coverage of 3 are close to the edges of the measurement domain. There, the light intensity is already rather low and the cameras cannot image the particles as sharply as in the center regions. This results in a higher number of segmented and short tracks, which posses a higher uncertainty. Within the central domain, where the particle image quality is much better, only a weak influence of the camera coverage on the uncertainties is observable. For those reliably reconstructed tracks, the estimated uncertainty

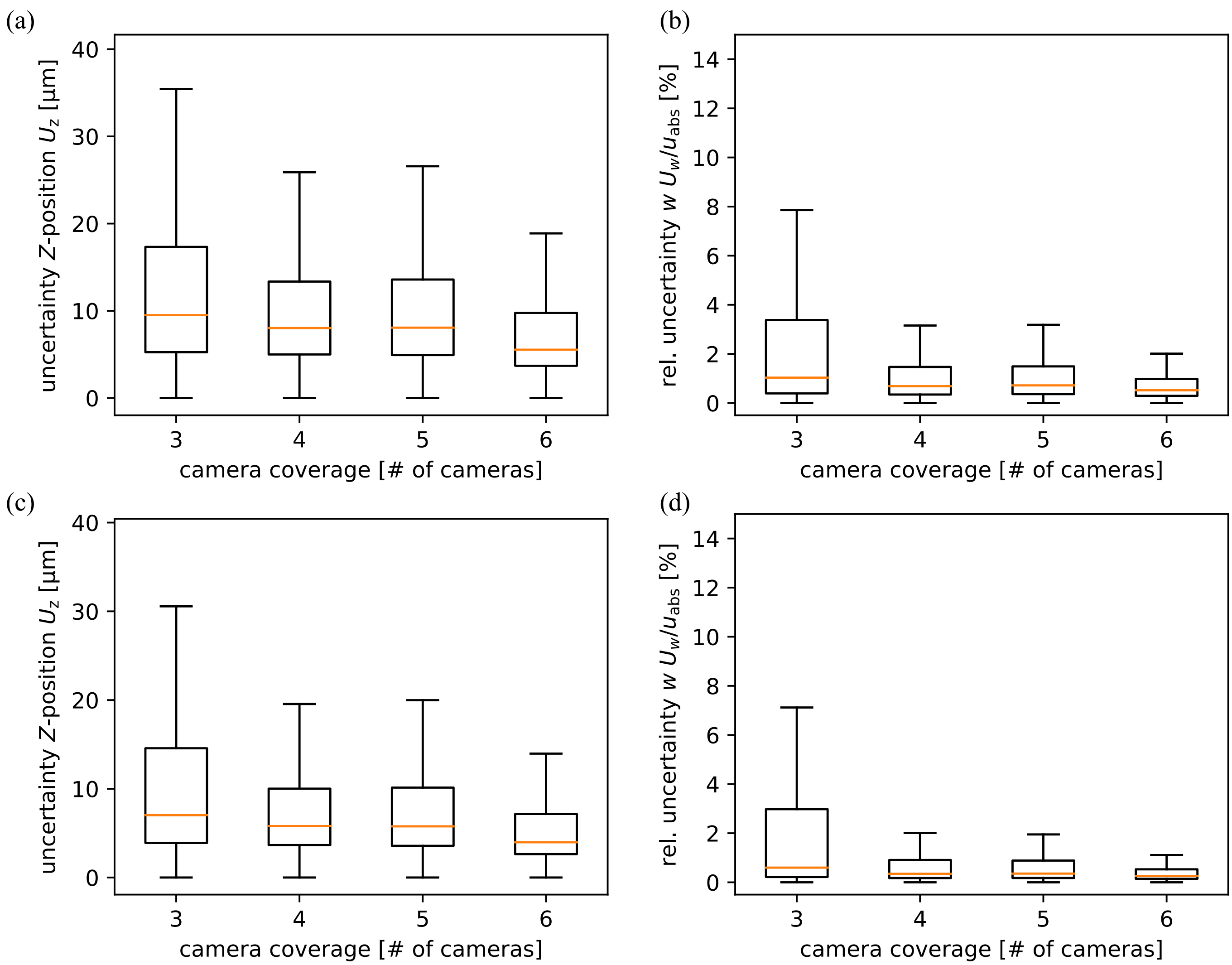

Figure 5. Box plot visualizations for the positional uncertainty distributions of the Z-component U_z (a and c) and the relative velocity uncertainty distributions for the Z-component U_w/u_abs (b and d). Compared are the estimated uncertainties stemming from 2nd order polynomial trajectory fits with a constant filter width of 11 time steps (a and b) and from 2nd order polynomial trajectory fits with an adaptive filter length (c and d).

is more dependent on the chosen polynomial filter length. Since the measured flow features a rather high dynamic range in the velocity values it is difficult to properly fit all trajectories with a single filter width. By employing the adaptive filter, the uncertainties can be decreased noticeably, indicating a much better local fit of the particle data.

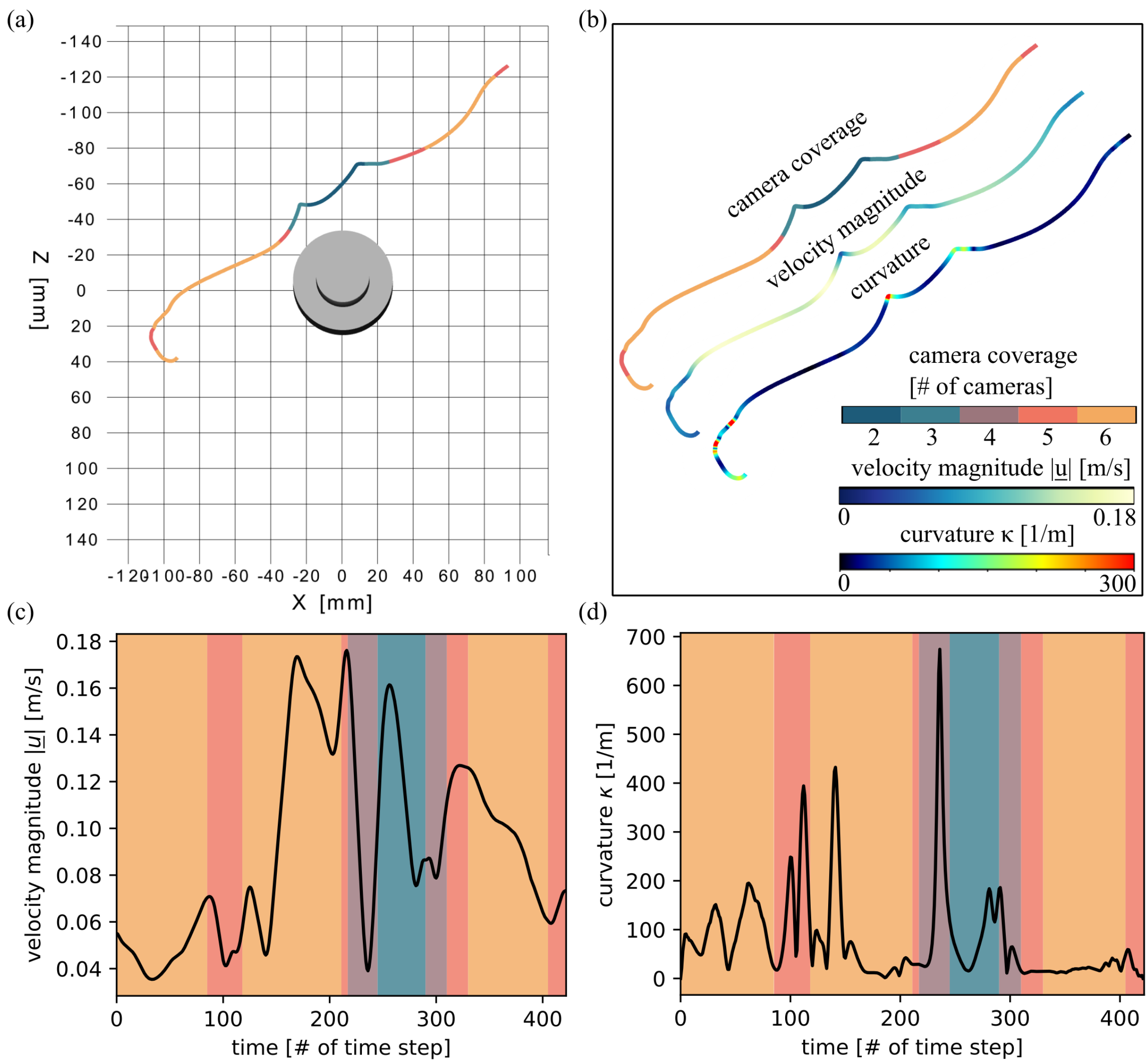

Figure 6. Exemplary investigation of a single particle trajectory crossing several camera coverage regions. (a) XZ plot of the trajectory showcasing its position withing the measurement domain. (b) Trajectory color-coded differently with the camera coverage, velocity magnitude and curvature along its temporal evolution. (c) Velocity magnitude plot over the temporal evolution. Background colors correspond to the camera coverage value. (d) Curvature plot over the temporal evolution. Background colors correspond to the camera coverage value.

After this global data set analysis, the following result will cover the study of a single particle trajectory. For this case study, a particle is selected, which has been tracked for a total of 422 out of all 500 time steps and which crosses regions of varying camera coverage. The chosen particle trajectory and its position in the measurement domain is illustrated in Figure 6 (a). When the particle was initially triangulated, it had a slow velocity and was located outside of the jet core region. Over time, the particle got entrained in the high-speed jet region, in which it got advected to the other end of the measurement volume. During the passage through the domain, the particle is observed by 6, 5, 6, 5, 3, 4, 5, 6 and finally 5 cameras. Now, the particle's velocity along the trajectory and the resulting track curvatures are being evaluated to verify, whether nonphysical discontinuities due to the changing number of involved cameras can be found. For a impression of the trajectory's characteristics, Figure 6 (b) shows the particle path color-coded with both considered quantities, the particle's velocity magnitude $|\underline{u}|$ and the local track curvature κ. The time evolution of these values are presented in Figure 6 (c) and (d). The background color in the two last mentioned figures represents the camera coverage values for each time step. Therefore, when discontinuities due to some reconstruction problems should be present, the would occur most likely, when the camera coverage value changes. But, both the velocity and the curvature plot do not show any sign of nonphysical particle motion at those crossing events. Some local minima/ maxima coincide with a change of the camera coverage but they can be linked to meaningful particle motions.

5. Conclusions

A volumetric flow measurement around a stepped cylinder was presented with the goal of validating the correct implementation of the novel object-aware Shake-the-Box approach. The measurement featured a multi-camera set-up and a view-obstructing stepped cylinder, resulting in regions, where a tracer can be seen by as few as three or by all six cameras. In order to obtain a continuous, artifact-free reconstruction result across those regions, the STB algorithm was informed about the cylinder by the incorporation of depth maps during the IPR sub-routine. Those depth maps were deduced from a CAD model of the object, fitted into the multi-camera system's coordinate system. The fitting of the CAD model to its correct position was possible by reconstructing stationary tracer particles attached to the object's surface. All necessary image processing and reconstruction steps were outlined to give a guideline for future measurements with a similar scope.

The discussed flow measurement results covered a brief description of the flow field around the complete object, both with respect to the particle trajectories and the interpolated, structured velocity field. For a further assessment of the reconstruction quality in dependency of the differently observed sub-regions, the estimated position and velocity uncertainties of all reconstructed particles were presented and discussed. It was found, that the median uncertainty is only weakly affected by the number of cameras involved in the reconstruction but the areas imaged by only three cameras show a much wider uncertainty distribution. But it was assumed, that this is mainly a factor of poor particle image signals in those outer measurement regions. Finally, a single trajectory traveling through a large portion of the measurement domain was selected for an investigating, whether nonphysical discontinuities can be observed while traveling through the different camera coverage regions. But no indications of erroneous reconstruction results at those crossings were found, when looking at the velocity and curvature values along the whole trajectory.

Overall, the conducted measurements validate the correct implementation of the novel OA-STB method and showcase the valid velocity field reconstruction all around the object of interest.

Acknowledgements

The author would like to acknowledge the support of Robert Brinkema during the set-up and the conduction of the experiment.

References

Crane, R. J., Popinhak, A. R., Martinuzzi, R. J., & Morton, C. (2022). Tomographic PIV investigation of vortex shedding topology for a cantilevered circular cylinder. *Journal of Fluid Mechanics*, *931*, R1. doi: 10.1017/jfm.2021.904

Hain, R., Kähler, C. J., & Michaelis, D. (2008). Tomographic and time resolved PIV measurements on a finite cylinder mounted on a flat plate. *Experiments in Fluids*, *45*(4), 715–724. doi: 10.1007/s00348-008-0553-x

Hendriksen, L. A., Sciacchitano, A., & Scarano, F. (2024). Object registration for 3D particle tracking. In *21th international symposium on the application of laser and imaging techniques to fluid mechanics.* Lisbon, Portugal.

Janke, T., & Michaelis, D. (2021). Uncertainty Quantification for PTV / LPT data and Adaptive Track Filtering. In *14th international symposium on particle image velocimetry.* Chicago, USA. doi: 10.18409/ispiv.v1i1.125

Perrin, R., Braza, M., Cid, E., Cazin, S., Chassaing, P., Mockett, C., … Thiele, F. (2008). Coherent and turbulent process analysis in the flow past a circular cylinder at high Reynolds number. *Journal of Fluids and Structures*, *24*(8), 1313–1325. doi: 10.1016/j.jfluidstructs.2008.08.005

Schanz, D., Gesemann, S., & Schröder, A. (2016). Shake-The-Box: Lagrangian particle tracking at high particle image densities. *Experiments in Fluids*, *57*(5), 70. doi: 10.1007/s00348-016-2157-1

Schanz, D., Novara, M., & Schröder, A. (2021). Shake-The-Box particle tracking with variable time-steps in flows with high velocity range (VT-STB). In *14th international symposium on particle image velocimetry.* Chicago, USA. doi: 10.18409/ispiv.v1i1.65

Wieneke, B. (2013). Iterative reconstruction of volumetric particle distribution. *Measurement Science and Technology*, *24*(2), 024008. doi: 10.1088/0957-0233/24/2/024008

Wieneke, B., & Rockstroh, T. (2024). Lagrangian particle tracking in the presence of obstructing objects. *Measurement Science and Technology*, *35*(5). doi: 10.1088/1361-6501/ad289d

Zhang, W., Daichin, & Lee, S. J. (2005). PIV measurements of the near-wake behind a sinusoidal cylinder. *Experiments in Fluids*, *38*(6), 824–832. doi: 10.1007/s00348-005-0981-9

Zhou, B., Wang, X., Guo, W., Gho, W. M., & Tan, S. K. (2015). Experimental study on flow past a circular cylinder with rough surface. *Ocean Engineering*, *109*, 7–13. doi: 10.1016/j.oceaneng.2015.08.062